ISSN 1063-7826, Semiconductors, 2009, Vol. 43, No. 11, pp. 1428–1432. © Pleiades Publishing, Ltd., 2009.
Original Russian Text © A.E. Belyaev, N.S. Boltovets, V.N. Ivanov, A.B. Kamalov, L.M. Kapitanchuk, V.P. Kladko, R.V. Konakova, Ya.Ya. Kudryk, V.V. Milenin, M.U. Nasyrov, P.V. Nevolin, 2009, published in Fizika i Tekhnika Poluprovodnikov, 2009, Vol. 43, No. 11, pp. 1468–1472.

SEMICONDUCTOR STRUCTURES, INTERFACES, AND SURFACES

Interphase Interactions and the Mechanism of Current Flow in Au–TiB$_x$–AuGe–*n*-GaP Ohmic Contacts

A. E. Belyaev[a], N. S. Boltovets[b], V. N. Ivanov[b], A. B. Kamalov[a], L. M. Kapitanchuk[c], V. P. Kladko[a], R. V. Konakova[a]^, Ya. Ya. Kudryk[a], V. V. Milenin[a], M. U. Nasyrov[a], and P. V. Nevolin[a]
[a] *Lashkaryov Institute of Semiconductor Physics, National Academy of Sciences of Ukraine, Kyiv, 03028 Ukraine*
^e-mail: konakova@isp.kiev.ua
[b] *State Research Institute Orion, Kyiv, 03057 Ukraine*
[c] *Paton Electric Welding Institute, National Academy of Sciences of Ukraine, Kyiv, 03680 Ukraine*

Submitted March 24, 2009; accepted for publication April 14, 2009

Abstract—Au–TiB$_x$–AuGe–*n*-GaP ohmic contacts have been investigated before and after rapid thermal annealing at $T = 723$, 773, and 873 K for 60 s in a hydrogen atmosphere. It is shown that the contact resistivity decreases with an increase in temperature in the range 77–232 K due to the thermionic nature of current flow in inhomogeneous ohmic contacts, while in the range 232–386 K the contact resistivity increases, which can be related to the conduction through metal shunts.

PACS numbers: 73.40.Cg, 73.40.Ns

DOI: 10.1134/S1063782609110062

1. INTRODUCTION

The technique for forming ohmic contacts plays an important role in the fabrication of semiconductor devices and integrated circuits (ICs), because the properties of ohmic contacts affect significantly such parameters of devices and ICs as noise, efficiency, and self-heating. The symmetry and linearity of current–voltage (*I*–*V*) characteristics in the absence of injection and minimum contact resistivity ρ_c reduce the heating and noise, which are related mainly to the contact phenomena, and increase the efficiency of light-emitting diodes and lasers. Obviously, all these advantages can be implemented only in a uniform contact, which implies primarily uniform stable metal/metal and metal/semiconductor interfaces.

Real contacts, especially to III–V semiconductors, are generally inhomogeneous; for example, ohmic contacts to GaP are formed mainly due to the interphase interactions at the metal–GaP interface [1–12]. Various processes may occur in this case: solid-phase epitaxy of, for example, silicon on GaP (Al–Si–Pd and Si–Pd ohmic contacts); formation of Pd_2GaP, $Pd_2Ga_xP_{1-x}$ [1], and $In_yGa_{1-y}P$ phases in the case of Pd–In contact [4]; and alloying with the formation of metal shunts (In–GaP contact) [3]. Depending on the doping level of *n*-GaP, the conditions for forming ohmic contacts, and the metallization type, ρ_c changes in a wide range (Fig. 1, Table 1).

To retard the processes of interphase interaction and mass transfer in metallization layers, especially on wide-gap semiconductors, diffusion barriers are used: buffer layers of metals or alloys, including interstitial alloys (interstitial phases) [11–14]. Recently, thin films of the best studied interstitial alloys—nitrides, borides, tungstates, and silicides of refractory metals—have been applied [11]. We have used for the first time amorphous TiB$_x$ films and titanium oxyborides as diffusion barriers in ohmic contacts to *n*-GaP [8, 9]. The Au–TiB$_x$–AuGe–*n*-GaP ohmic contacts (carrier concentration $\approx 10^{17}$ cm^{-3} in *n*-GaP) were found to

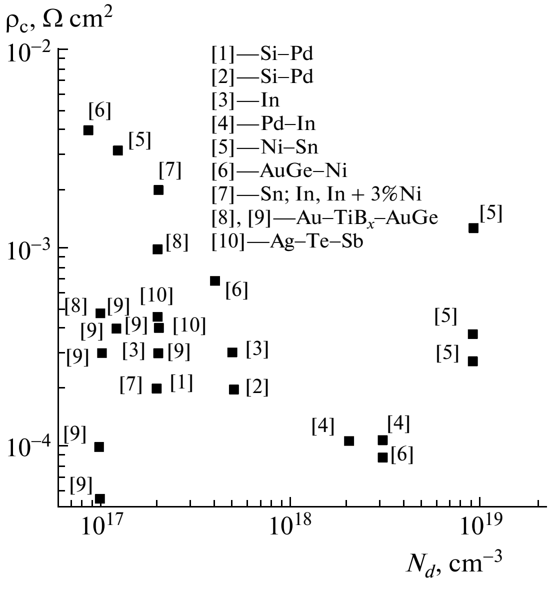

Fig. 1. Dependence of ρ_c on the *n*-GaP's doping level and metallization type [1–10].

Table 1. Dependence of ρ_c on the n-GaP doping level and annealing conditions [1–10, 12]

Metallization	Dopant concentration, cm^{-3}	Annealing temperature T (in °C) and time	Contact resistivity ρ_c, Ω cm^2	Reference	Notes
Si–Pd	5×10^{17}	400–600, 30 min	2×10^{-4}	[1]	Solid-phase epitaxy of Si on GaP and formation of the Pd_2GaP and $Pd_2(Ga_xP_{1-x})$ phases
Si–Pd	5×10^{17}	400–650	2×10^{-4}	[2]	Metal shunts
In	$(2–4) \times 10^{17}$	580, 5 min	2.8×10^{-4}	[3]	Formation of the $In_yGa_{1-y}P$ phase
Pd–In	$(2–3) \times 10^{18}$	600, 1 min	10^{-4}	[4]	
Ni–Sn	1.2×10^{17}	500–600, 2 min	$5.9–3.3 \times 10^{-3}$		
Ni–Sn	9×10^{18}	500–600, 2 min	$1.3 \times 10^{-3}–2.7 \times 10^{-4}$	[5]	
Ag	1.6×10^{17}	650, 5 min	6.1×10^{-2}		
In–Ni	10^{17}	500, 0.5 min	5×10^{-3}		
Au–Ge–Ni	$8.5 \times 10^{16}–3 \times 10^{18}$	600, 2 min	$4 \times 10^{-3}–9 \times 10^{-5}$	[6]	
Sn	$(2–10) \times 10^{17}$	600, 10 min	2×10^{-3}		
In	$(2–10) \times 10^{17}$	500, 5 min	10^{-3}	[7]	
In + 3%Ni	$(2–10) \times 10^{17}$	500, 5 min	2×10^{-4}		
Au–TiB$_x$–	10^{17}	510, 0.5 min	$4.8 \times 10^{-4}–4 \times 10^{-4}$	[8]	
AuGe	$(2–4) \times 10^{17}$	510, 1 min	3.3×10^{-4}	[9]	
Ag–Te–Sb	2×10^{17}	700, 3 min	4×10^{-4}	[10]	
Au–TiB$_x$–AuGe	10^{17}	600, 1 min	1.1×10^{-4}	[12]	

have a resistivity of ~(1.1–4) × 10^{-4} Ω cm^2, which did not change after a 2 year storage at room temperature in air. This fact indicates a high stability of the TiB$_x$ diffusion barrier, AuGe–n-GaP interface, and the AuGe layer (forming the ohmic contact). At the same time, the thermal stability of this metallization and the properties of Au–TiB$_x$–AuGe–n-GaP ohmic contacts subjected to rapid thermal annealing (RTA), imitating both some modes of ohmic contact formation and short-term thermal loads (for example, superheating during operation), have barely been investigated. We consider below the interphase interactions and mechanism of current flow in these ohmic contacts.

2. EXPERIMENTAL

In this paper, we report the results of studying the electrical parameters of Au–TiB$_x$–AuGe–n-GaP ohmic contacts before and after RTA at $T = 723$, 773, and 873K for 60 s in a hydrogen atmosphere. Before and after RTA, we investigated the depth profiles of the ohmic contact's components by Auger electron spectroscopy, analyzed the phase composition of the metallization by X-ray diffractometry, and measured the temperature dependences of the contact resistivity ρ_c (which were used to determine the barrier height and nature of current flow).

The ohmic contacts were formed by magnetron sputtering of the metallization components in the same cycle on a cold wafer from a Czochralski-grown n-GaP single crystal. The n-GaP wafer was ~400 μm thick and had a dopant (tellurium) concentration of ~10^{17} cm^{-3}. The dislocation density did not exceed 10^5 cm^{-2}. Before deposition of metallization layers the GaP surface was subjected to photon cleaning. The layer thicknesses were as follows: Au(500 Å)–TiB$_x$(500 Å)–Au(400 Å)–Ge(100 Å)–n-GaP. The contact resistivity was measured by the radial transmission line's modeling method with a constant ratio (7.4) of the internal and external radii of contact areas [15] in the temperature range 80–380 K. A mask with contact areas having internal radii of 20, 40, 60, 80, and 100 μm was used.

3. RESULTS

The layered metallization structure was found to be retained after RTA (Figs. 2a–2d). However, RTA at $T = 873$ K led to a significant expansion of the interphase interaction in the region in the AuGe–n-GaP contact with conservation of the buffer properties of the TiB$_x$ layer, which was characterized by a high oxygen content both in the initial state and after RTA. The X-ray diffraction data indicate the presence of a quasi-amorphous TiB$_x$ layer in all contacts under study. The

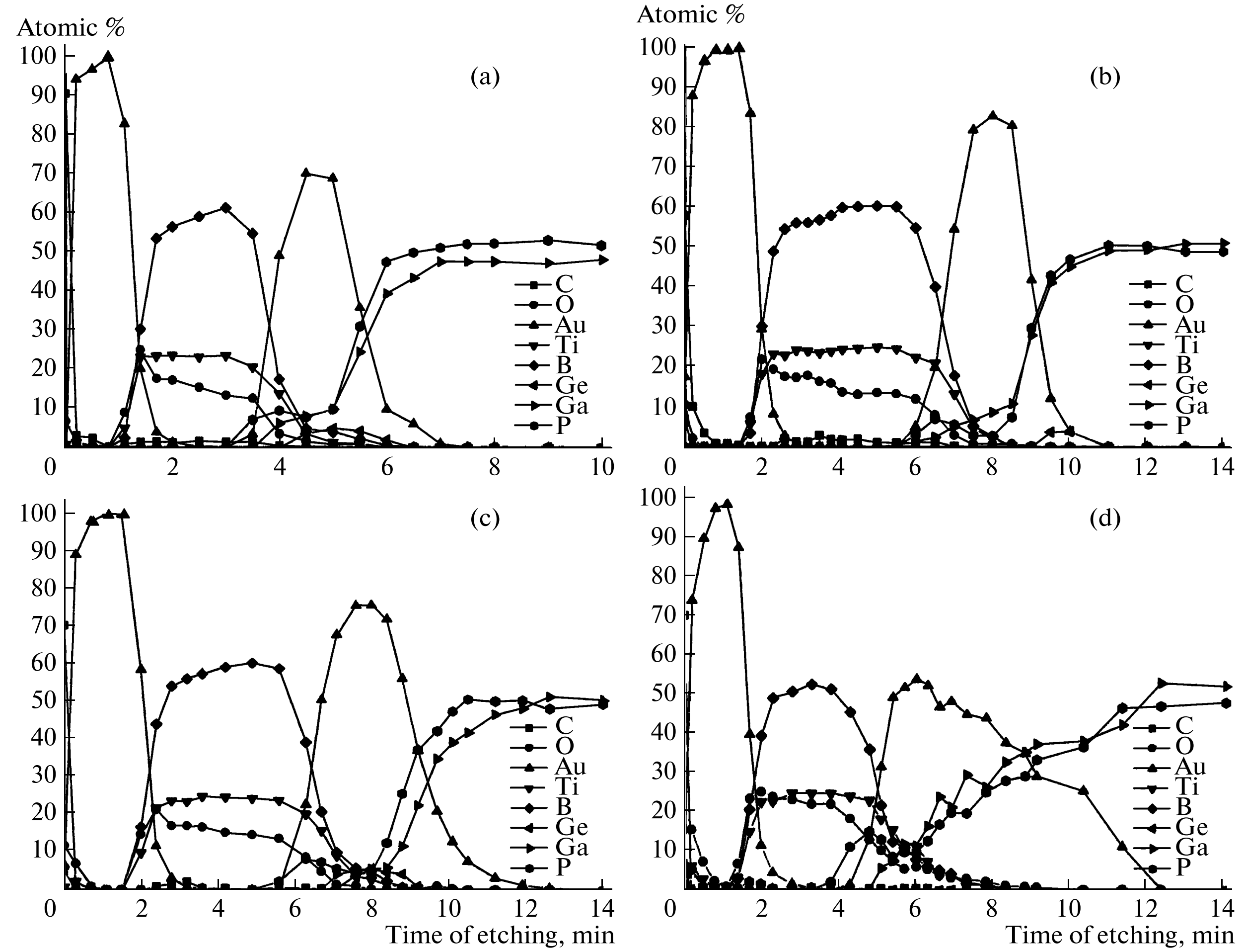

Fig. 2. Component depth profiles in the Au–TiB$_x$–AuGe–n-GaP ohmic contact (a) before and (b–d) after RTA at T = (b) 723, (c) 773, and (d) 873 K.

diffraction patterns of both the initial sample and the samples subjected to RTA at 723 and 773 K exhibited, along with Au, small amounts of $AuGa_2$, $AuGaO_2$, GeP_3, and Ge; in addition, the $Au_{0.72}Ge_{0.28}$ phase was formed after RTA at 873 K. Concerning the electrical characteristics of these contacts, the initial sample had rectifying properties. After RTA at T = 723 K, the I–V characteristics were found to be symmetric and linear. In this case, the contact resistivity ρ_c, measured at T = 300 K, was ~ (5–6) × 10^{-3} Ω cm^2. RTA at T = 773 and 873 K led to a decrease in ρ_c to ~ (3–4) × 10^{-4} and (1–5) × 10^{-5} Ω cm^2, respectively. The spread of ρ_c over the wafer area of half an order of magnitude indicates the presence of an inhomogeneous conducting layer forming an ohmic contact with n-GaP. Taking into account this factor, the temperature dependences of ρ_c were measured on the test samples annealed at 723 and 773 K. The results obtained are shown in Fig. 3. They indicate that in the temperature range 77–232 K ρ_c decreases with an increase in T, and the temperature dependences of ρ_c for both samples can be described by two exponentials (each curve has two slopes) with different activation energies (barrier heights φ_B), which is characteristic of a thermionic current flow with a nonuniform current distribution over the contact area. For the sample annealed at T = 723 K, the activation energies in the temperature dependences of ρ_c are ~0.092 and ~0.04 eV in the temperature range 77–90 and 90–232 K, respectively. In the case of RTA at 500°C, the activation energies decreased and the temperature range changed for both portions. Specifically, the activation energies were ~0.083 and ~0.035 eV in the ranges T = 77–116 and 116–232 K, respectively. This fact indicates the incompleteness of physicochemical processes at the AuGe–n-GaP interface after RTA at T = 723 K and their enhancement after annealing at 773 K.

Note also that ρ_c increases with an increase in temperature from 232 to 386 K in the sample annealed at T = 723 K. In the case of RTA at T = 773 K, ρ_c also increases in the same temperature range, but much more slowly than after RTA at T = 723 K. The increase in ρ_c with increasing temperature, as was shown for an alloyed In–GaP ohmic contact [3] and for an alloyed

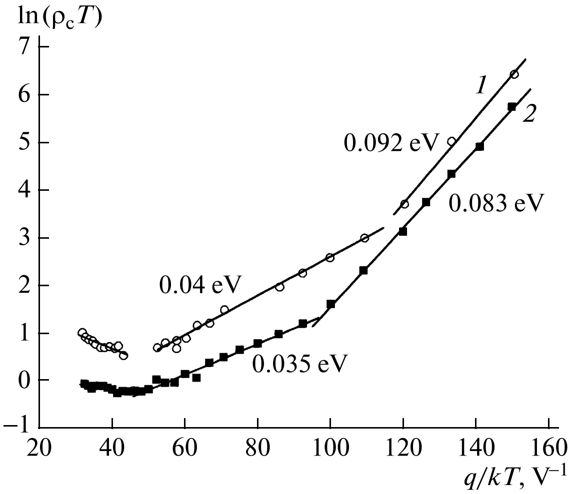

Fig. 3. Temperature dependences of the contact resistivity in the thermionic emission coordinates after RTA at T = (*1*) 723 and (*2*) = 773 K.

In–GaN ohmic contact [16, 17], can be related to the metal shunts formed at structural defects in the near-contact semiconductor layer; in particular, at growth dislocations.

The nature of these shunts can be related to the thermal stress in the contacts caused by the difference of the thermal expansion coefficients of the semiconductor and metal (alloy) forming the contact. For example, in the case under consideration, the thermal expansion coefficients α for GaP, Au, and Ge are 5.6×10^{-6}, 14.2×10^{-6}, and 4.5×10^{-6} K^{-1}, respectively. The gold's mass transfer through the polycrystalline 10-nm-thick Ge film (Fig. 2) in the thin Au layer at the interface with GaP upon sample cooling to room temperature (for example, after RTA at T = 723 K) induces a thermal stress $\sigma_{Au} = (\alpha_{Au} - \alpha_{GaP})\Delta T \frac{E_{Au}}{1 - \nu_{Au}}$ (here, E = 78 GPa is Young's modulus of Au, $\nu_{Au} = 0.4$ is the Poisson ratio of Au, and $\Delta T = 723 - 300 = 423$ K), which is about 4.7×10^8 Pa at a GaP ultimate strength of 10^9 Pa [18] and Au ultimate strength of $\approx 7.8 \times 10^8$ Pa (the ultimate strength of materials is two orders of magnitude smaller than the modulus of elasticity [19]). The stress can also be caused by the misfit between the GaP lattice's parameter (0.545 nm), gold's atomic radius (0.144 nm), and the lattice constants of the $AuGaO_2$ and $AuGa_2$ (0.67 nm) compounds, which can be formed during RTA. The relaxation of thermal stress and misfit strain may increase the density of structural defects in the near-contact GaP region and enhance shunt formation.

Table 2. Gold resistivity ρ_{Au}, shunt resistance R_{sh}, contact resistivity ρ_c, and the number of shunts per unit area N at different temperatures

T, K	ρ_{Au}, Ω cm	R_{sh}, Ω	ρ_c, Ω cm^2	N
289	2.15×10^{-6}	2.3×10^3	5.6×10^{-3}	4×10^5
300	2.26×10^{-6}	2.4×10^3	6×10^{-3}	4×10^5
350	2.68×10^{-6}	2.9×10^3	6.6×10^{-3}	4.4×10^5
386	3×10^{-6}	3.2×10^3	7×10^{-3}	4.6×10^5

The resistance of one of the shunts in the sample subjected to RTA at 723 K was calculated according to the model proposed in [3]. In accordance with [3], we assume that the shunt radius is of the same order of magnitude as the GaP lattice's constant (0.545 nm) and that the shunt consists of gold. Then, the shunt resistance $R_{sh} = \rho_{Au} l/S$, where ρ_{Au} is the Au resistivity (2.2×10^{-6} Ω cm at 283 K). The temperature coefficient of the Au resistivity at 293 K is 3.9×10^{-3} K^{-1} [20]. Let the shunt length l be equal to the space-charge layer's width W. At zero bias $W = \sqrt{2\varepsilon_0\varepsilon(V_d - kT/q)/qN_d}$ is ~10^{-5} cm and changes only slightly in the temperature range where metallic conductivity is observed in the ohmic contact. Here, ε = 11.1 is the GaP permittivity, $\varepsilon_0 = 8.85 \times 10^{14}$ F/cm is the permittivity of free space, V_d is the diffusion potential at the Au–GaP interface, and $N_d = 10^{17}$ cm^{-3} is the uncompensated donor concentration in GaP.

The calculation results listed in Table 2 indicate that in the range T = 289–386 K the number of shunts changes insignificantly and exceeds the dislocation density in the initial GaP by about half an order of magnitude, which is apparently related to the additional formation of shunts at the structural defects generated in the sample annealed at 723 K upon its cooling to T = 300 K.

The specific features of the temperature dependence of ρ_c after RTA at 773 K are apparently related to the decrease in the barrier height in the ohmic contact due to the Ge diffusion in GaP and formation of a thin Ge-doped layer of n type with a higher concentration of donors, which decrease the barrier height but retain the thermionic current flow in the contact, and the competition between the processes of current flow through the shunts and thermionic emission.

4. CONCLUSIONS

Thus, based on the study of the temperature dependence of ρ_c and interphase interactions in Au–TiB_x–AuGe–n-GaP ohmic contacts after RTA at T = 723 and 773 K, it is shown that ρ_c decreases with an increase in temperature in the range 77–232 K, which is due to the thermionic current flow through the inhomogeneous ohmic contact, as is evidenced by the presence of two slopes in the dependence $\ln(\rho_c T) = f(q/kT)$, whereas in the range 232–386 K, ρ_c increases with an increase in temperature; this is inconsistent with the typical mechanisms of the current flow in contacts and is related to the conduction through metal shunts, which were reviewed previously in alloyed In–GaP(GaN) contacts by Blank et al. [3, 16, 17]. However, in contrast to [3, 16, 17], the metal shunts in the case under study are formed not upon alloying but via the diffusion Au transfer through structural defects (possibly, microdiscontinuities).

REFERENCES

1. M. H. Park, L. S. Wang, D. C. Dufner, Fei Deng, S. S. Lau, I. H. Tan, and F. Kish, J. Appl. Phys. **81**, 3138 (1997).
2. L. S. Wang, M. H. Park, H. A. Jorge, I. H. Tan, and F. Kish, Electron. Lett. **82**, 409 (1996).
3. T. V. Blank, Yu. A. Gol'dberg, O. V. Konstantinov, V. G. Nikitin, and E. A. Posse, Pis'ma Zh. Tekh. Fiz. **30** (19), 17 (2004) [Tech. Phys. Lett. **30**, 806 (2004)].
4. C. F. Lin, D. B. Ingerly, and Y. A. Chang, Appl. Phys. Lett. **69**, 3543 (1996).
5. I. G. Vasil'ev, G. G. Boeva, V. N. Kurasov, I. V. Ryzhikov, and I. I. Kruglov, Élektron. Tekhn., Ser. Poluprovodn. Prib. **3**, 65 (1970).
6. K. K. Shin and J. M. Blum, Solid State Electron. **15**, 1177 (1972).
7. R. S. Ignatkina, R. N. Krivosheeva, S. S. Meskin, V. N. Ravich, and N. F. Sil'vestrova, Prib. Tekh. Eksp. **5**, 215 (1968).
8. A. E. Belyaev, N. S. Boltovets, V. N. Ivanov, R. V. Konakova, Ya. Ya. Kudryk, V. V. Milenin, M. U. Nasyrov, and P. V. Nevolin, in *Proc. 17th Int. Symp. on Radiation Physics of Solids, Sevastopol', Ukraine, 2008* (MGIÉM, Moscow, 2008), p. 194.
9. A. E. Belyaev, N. S. Boltovets, V. N. Ivanov, A. B. Kamalov, L. N. Kapitanchuk, V. P. Klad'ko, R. V. Konakova, Ya. Ya. Kudrik, V. V. Milenin, M. U. Nasyrov, and P. V. Nevolin, in *Proc. Int. Conf. on Sci.-Techn. Progress and Modern Aviation* (Baku, Azerbaijan, 2009), p. 283.
10. H. Nakatsuka, A. J. Domenico, and G. L. Pearson, Solid State Electron. **14**, 849 (1971).
11. O. A. Ageev, A. E. Belyaev, N. S. Boltovets, R. V. Konakova, V. V. Milenin, and V. A. Pilipenko, *Interstitial Phases in Technology of Semiconductor Devices and VLSI Circuits* (Inst. for Single Crystals, Khar'kov, 2008) [in Russian].
12. A. E. Belyaev, N. S. Boltovets, V. N. Ivanov, V. P. Klad'ko, R. V. Konakova, Ya. Ya. Kudryk, V. V. Milenin, and V. N. Sheremet, SPQEO **11**, 209 (2008).
13. A. G. Baca, F. Ren, J. C. Zolper, R. D. Briggs, and S. J. Pearton, Thin Solid Films **308–309**, 599 (1997).
14. T. V. Blank and Yu. A. Gol'dberg, Fiz. Tekh. Poluprovodn. **41**, 1281 (2007) [Semiconductors **41**, 1263 (2007)].
15. A. N. Andreev, M. G. Rastegaeva, V. P. Rastegaev, and S. A. Reshanov, Fiz. Tekh. Poluprovodn. **32**, 832 (1998) [Semiconductors **32**, 739 (1998)].
16. T. V. Blank, Yu. A. Gol'dberg, O. V. Konstantinov, V. G. Nikitin, and E. A. Posse, Fiz. Tekh. Poluprovodn. **40**, 1204 (2006) [Semiconductors **40**, 1173 (2006)].
17. V. N. Bessolov, T. V. Blank, Yu. A. Gol'dberg, O. V. Konstantinov, and E. A. Posse, Fiz. Tekh. Poluprovodn. **42**, 1345 (2008) [Semiconductors **42**, 1315 (2008)].
18. S. S. Strel'chenko and V. V. Lebedev, *III–V Compounds: Handbook* (Metallurgiya, Moscow, 1984) [in Russian].
19. Yu. A. Kontsevoi, Yu. M. Litvinov, and É. A. Fattakhov, *Plasticity and Hardness of Semiconductor Materials and Structures* (Radio i Svyaz', Moscow, 1985).
20. H. Kuhling, *Handbook of Physics* (Fachbuchverlag, Leipzig, 1965; Mir, Moscow, 1985).

Translated by Yu. Sin'kov